SCISPACE
formerly Typeset

Open access • Journal Article • DOI:10.1016/J.MSEA.2018.11.065

Into the quenching & partitioning of a 0.2C steel: An in-situ synchrotron study

— Source link

Pierre Huyghe, Matteo Caruso, Jean Louis Collet, Sylvain Dépinoy ...+1 more authors

Institutions: Université libre de Bruxelles

Published on: 16 Jan 2019 - Materials Science and Engineering A-structural Materials Properties Microstructure and Processing (Elsevier)

Topics: Bainite, Austenite, Quenching, Martensite and Carbon

Related papers:

- Atomic-scale analysis of carbon partitioning between martensite and austenite by atom probe tomography and correlative transmission electron microscopy
- Phase Transformations in Steels during Quenching and Partitioning Heat Treatment
- Effects of Q&P Processing Conditions on Austenite Carbon Enrichment Studied by In Situ High-Energy X-ray Diffraction Experiments
- Quenching and partitioning : a new steel heat treatment concept
- Microstructural development during the quenching and partitioning process in a newly designed low-carbon steel

Share this paper:

View more about this paper here: https://typeset.io/papers/into-the-quenching-partitioning-of-a-0-2c-steel-an-in-situ-3yyfblflw6

Materials Science & Engineering A 701 (2017) 254–263

Contents lists available at ScienceDirect

Materials Science & Engineering A

journal homepage: www.elsevier.com/locate/msea

On the relationship between the multiphase microstructure and the mechanical properties of a 0.2C quenched and partitioned steel

Pierre Huyghe[a,*], Loic Malet[a], Matteo Caruso[b], Cédric Georges[b], Stéphane Godet[a]

[a] 4MAT, Materials Engineering, Characterization, Processing and Recycling, Université Libre de Bruxelles, 50 Avenue FD Roosevelt, CP194/03, B-1050 Brussels, Belgium
[b] CRM – CRM Group, Avenue du Bois Saint Jean 21 P59, B-4000 Liège, Belgium

ARTICLE INFO

Keywords:
Quenching and partitioning
Austempering
Phase quantification
Retained austenite
Mechanical properties

ABSTRACT

In the present work, Quenching and Partitioning (Q & P) heat treatments were carried out in a quench dilatometer on a 0.2 wt% carbon steel. The microstructure evolution of the Q & P steels was characterized using dilatometry, SEM, EBSD and XRD. The martensitic transformation profile was analyzed in order to estimate the fraction of martensite formed at a given temperature below the martensite start temperature M_s. Q & P was shown to be an effective way to stabilize retained austenite at room temperature. However, the measured austenite fractions after Q & P treatments showed significant differences when compared to the calculated values considering ideal partitioning conditions. Indeed, the measured austenite fractions were found to be less sensitive to the quench temperature and were never larger than the ideal predicted maximum fraction. Competitive reactions such as austenite decomposition into bainite and carbide precipitation were found to occur in the present work.

Furthermore, a broad range of mechanical properties was obtained when varying the quenching temperatures and partitioning times. The direct contributions between Q & P microstructural constituents -such as retained austenite as well as tempered/fresh martensite- and resulting mechanical properties were scrutinized. This was critically discussed and compared to quenching and austempering (QAT) which is a more conventional processing route of stabilizing retained austenite at room temperature. Finally, Q & P steels were shown to exhibit an interesting balance between strength and ductility. The achievement of this interesting combination of mechanical properties was reached for much shorter processing times compared to QAT steels.

1. Introduction

The automotive industry is mainly driven by requirements regarding the vehicle safety and the greenhouse gas emissions. Requirements on safety considerations have increased with the introduction of several test protocols by vehicle regulatory organizations. Simultaneously, vehicle manufacturers have to deal with issues such as environment, greenhouse gas emissions and fuel consumption. Amongst the different proposed strategies, the use of lightweight materials seems to offer the most promising advantages [1]. In order to stay competitive with respect to emerging materials such as Al-or Mg-alloys, polymers or composites, the steel industry has to continuously evolve and innovate. Therefore, complex steels in terms of processing, compositions and microstructures were introduced and called advanced high strength steels (AHSS) [2,3].

Over the last 10 years, an increasing research effort has been carried out on the development of these advanced high strength steels. The first generation of AHSS refers to Dual Phase (DP), Transformation Induced Plasticity (TRIP), and Martensitic (M) steels. The second generation of AHSS consists of austenitic steels such as Twinning-Induced Plasticity (TWIP) steels [2,3]. The third generation of AHSS produced by Quenching and Partitioning (Q & P) was proposed by Speer et al. in 2003 as a novel heat treatment in order to produce steels with improved strength-ductility combinations [4–6]. The third generation is meant to provide a better strength-ductility compromise than the first generation with lower cost than the second generation.

The Quenching and Partitioning process (Q & P) consists, first, of an interrupted quench between the martensite-start temperature and the martensite-finish temperature from intercritical annealing or full austenitization in order to form controlled fractions of martensite. This is followed by a partitioning step in order to stabilize the untransformed austenite at room temperature through carbon enrichment [5]. In order to maximize the carbon transfer from martensite to austenite, the use of specific alloying elements and the design of appropriate Q & P parameters are required to eliminate or minimize competing phenomena such as carbide formation and austenite decomposition [4,7]. The

* Corresponding author.

http://dx.doi.org/10.1016/j.msea.2017.06.058
Received 23 February 2017; Received in revised form 12 June 2017; Accepted 13 June 2017
Available online 17 June 2017
0921-5093/ © 2017 Elsevier B.V. All rights reserved.

microstructure produced, using full austenitization, ideally consists of carbon-depleted lath martensite and significant fractions of retained austenite providing an improved combination of strength and ductility [2].

Although intense research has been carried out on the effect of composition and Q & P parameters on the microstructure and mechanical properties of Q & P steels [7–20], quantitative evaluation of the complex microstructures remains difficult and, moreover, establishing a direct correlation between Q & P microstructural constituents and resulting mechanical properties remains a real challenge.

As the initial interrupted quench is achieved at a temperature Q_T between the martensite start temperature and the martensite finish temperature, the microstructure undergoing the partitioning step is a mixture of controlled fractions of martensite and untransformed austenite. Consequently, the microstructural evolution that will take place during partitioning will be a combination of carbon partitioning, and potentially other mechanisms occurring during tempering of martensite and the austempering of austenite. Therefore, complex microstructures are obtained through the Q & P process and require refined microstructural characterization. The present work is a contribution to phase quantification in Q & P steels and a better understanding of its direct correlation to the resulting mechanical properties. In order to gain further insights into the link between process parameters, microstructure development and related properties, the Q & P process is systematically compared to the quenching and austempering (QAT) process. Indeed, the QAT process has been exclusively studied in the context of the development of Transformation Induced (TRIP) multiphase steels in recent years.

2. Experimental procedures

The material investigated is a 0.8 mm thick cold-rolled metal sheet whose composition (in wt%) and critical temperatures are given in Table 1. After reheating at 1250 °C for 1 h, rolling blocks (160 mm length*60 mm width*60 mm thickness) were cut from the heat blocks. First, the blocks were hot rolled from 60 mm thick to 3 mm. Then the 3 mm-thick sheets were cold-rolled in several passes to 0.8 mm-thick sheets. The received microstructure prior to the following experiments is composed of ferrite plus pearlite. The transformation temperatures were measured by dilatometry using the following thermal schedule: the specimen is first fully austenitized at 900 °C for 5 min at a heating rate of 10 °C/s, before being quenched at room temperature at a cooling rate of 50 °C/s.

Dilatometry samples with 10*4*0.8 mm^3 dimensions were stamped from the as-received steel sheet. The rolling direction is parallel to the longest side. In order to optimize the dilatometry signal, the sides were ground with 500 grit SiC grinding paper. The DIL805A Bahr quench dilatometer was operated under vacuum (10^{-4} mbar). Induction heating was used while controlled cooling was achieved using He gas. The temperature was recorded using a *S* thermocouple welded on the sample.

The thermal schedules are plotted in Fig. 1. In the present work, the quenching and austempering process (QAT) is used as a reference as the microstructure is fully austenitic prior the isothermal holding step at 400 °C. The processes have the same austenitization conditions as well as the same heating and cooling rates. Regarding the Q & P procedure, the quenching temperature Q_T and the partitioning time P_t are the parameters investigated, while it is the austempering time A_t for the QAT process.

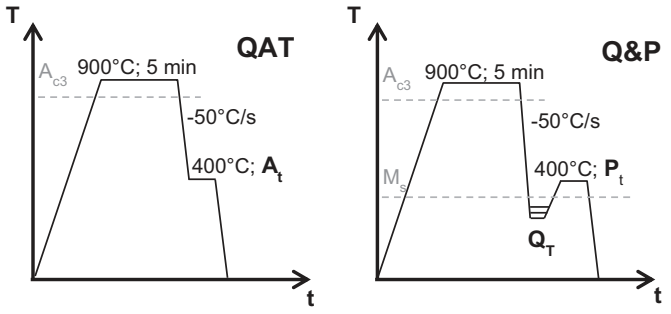

Fig. 1. Schematic thermal profiles: QAT = quenching & austempering, Q & P = quenching & partitioning. A_t = austempering time, Q_T = quenching temperature, P_t = partitioning time.

Microstructural characterization was performed on the section containing the RD and ND directions. Classical polishing methods were used to prepare the metallographic sections. The specimens were ground and then polished down to 1 μm with diamond paste. LePera color etching technique was used for optical microscopy observations [21]. The etchant is composed of two different solutions: a mixture of 1% sodium metabisulfite ($Na_2S_2O_5$) in water and 4% picric acid in ethyl alcohol. The two solutions were mixed in a 1:1 volume ratio before being used.

SEM characterization was conducted on a Hitachi FEG-SEM using a voltage of 20 kV. Samples for SEM characterization were etched in 2% Nital for approximately 10 s. EBSD was conducted on the same FEG-SEM equipped with an EBSD detector containing a phosphor screen and a CCD camera. The EBSD data was recorded using at an accelerating voltage of 20 kV, tilt angle of 70°, working distance of 15 mm and a step size of 80 nm. A final polishing step using 0.05 μm colloidal silica was used prior to EBSD. Post processing of the Kikuchi patterns was achieved using TSL OIM analysis software. The volume fraction and the carbon concentration of retained austenite were measured at room temperature using a D8 Advance diffractometer with Cu K_α radiation. X-Ray diffraction experiments were achieved using acceleration voltage of 40 kV, a current of 25 mA and spinning at 10 rpm. The measurements were performed in the diffraction angle (2θ) range of $40° - 100°$ using a step size of 0.015° and a counting time per step of 3 s. The retained austenite volume fraction was determined with the direct comparison method [22,23] using the integrated intensity of the $(200)_\alpha$, $(211)_\alpha$, $(220)_\gamma$ and $(311)_\gamma$ peaks. The carbon concentration of the retained austenite was calculated from the austenite lattice parameter obtained from the peak positions as described in the work of Van Dijk and coworkers [24].

Tensile tests were conducted on a 30 K Lloyd machine equipped with an extensometer with a gauge length of 25 mm for strain measurements. Tensile specimens were heat treated in molten salt baths, and machined by Electrical Discharge Machining, with the tensile axis in the rolling direction. The initial gauge length was 50 mm and the width 12.5 mm. Tests were performed at a strain rate of 10^{-4}/s. 0.2% yield strength (YS), ultimate tensile strength (UTS) and uniform elongation (UEl) were obtained and averaged from 3 tests. Moreover, in order to study the work-hardening behavior of the heat treated samples, the instantaneous work-hardening exponent was calculated from the tensile curves using the following equation:

$$n = \frac{d(\ln \sigma)}{d(\ln \varepsilon)} \quad (1)$$

Table 1
Chemical composition (in wt%) and measured critical temperatures (°C) of the investigated steel.

C	Si	Mn	Cr	P	S	N	Fe	A_{c3}	A_{c1}	M_s
0.197	1.405	2.308	0.205	0.003	0.002	0.005	balance	853 ± 6	754 ± 5	370 ± 7

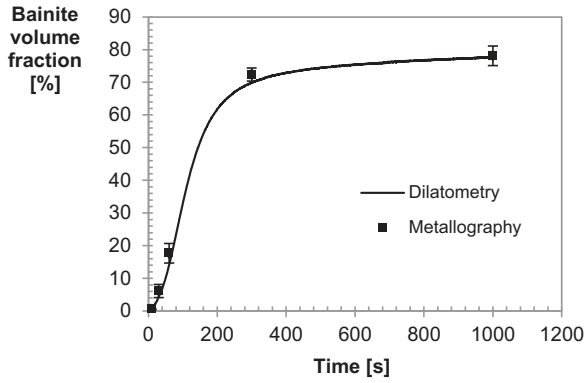

Fig. 2. Bainite fraction as a function of austempering time at 400 °C: the continuous line corresponds to the estimated bainite fraction from dilatometry curve and the squares are volume fractions measured using LePera color etching.

where σ is the true stress and ε is the true strain.

3. Results

3.1. Bainitic and martensitic transformation

Assuming that the volume fractions of martensite and bainite are proportional to the change in length, their volume fractions at different temperatures and different holding times can be extracted from dilatometry curves.

The bainitic matrix in QAT steels is formed during the austempering step at 400 °C and its volume fraction depends on the austempering time. Dilatometry revealed an expansion of around 0.5% when austempering at 400 °C for 1000 s. Combining dilatometry and color etching analysis allows the quantification of bainite fraction as a function of austempering time as can be seen in Fig. 2. Hence, assuming no variation of the austenite lattice parameter during the bainitic transformation, the fraction of bainite $V_B(t)$ at a given time t can be computed using a simple lever rule,

$$V_B(t) = V_B^{fin} \cdot \frac{l(t) - l_0}{l_{fin} - l_0} \quad (2)$$

where V_B^{fin} is the volume fraction of bainite formed after 1000 s austempering and that was determined using metallography, l_{fin} is the length recorded after 1000 s while l_0 and $l(t)$ are the initial length before transformation and the length at time t, respectively.

The evolution of the bainite fraction was followed by metallography using LePera color etching as can be observed in Fig. 3. In this Figure, bainite is blue and light brown and its volume fraction increases with the austempering time. This is also reported in Fig. 2. There is a good agreement between the bainite fractions obtained by metallography and those computed using Eq. (2).

The fractions of initial martensite formed at a temperature between the martensite-start temperature M_s and the martensite-finish temperature M_f were determined by using the lever rule applied to the martensitic transformation profile on the dilatometry curve [25]. These calculated initial martensite fractions are plotted in Fig. 4. They are confirmed by metallography as presented in Fig. 5. Samples were austenitized at 900 °C for 5 min before being quenched at various temperatures Q_T namely 300 °C, 320 °C, 340 °C and 360 °C for 5 s. These temperatures are below M_s that is 370 °C for this steel. Specimens were finally quenched to room temperature. When the quenching temperature decreases, the fraction of etched areas increases. It corresponds to the auto-tempered martensite formed at a given Q_T. In parallel, the smooth unetched areas that correspond to untempered martensite/retained austenite islands increase with the quenching temperature [26,27]. Holding times at given quenching temperatures were kept short in order to avoid the formation of undesirable additional transformation products.

3.2. Austenite stabilization at room temperature

The volume fractions of retained austenite were measured by X-ray diffraction for different quenching temperatures (280 °C, 320 °C and 360 °C) and for different partitioning times (10 s, 120 s and 1000 s) as represented in Fig. 6a. The austenite fractions measured by XRD are compared to the solid curve representing the predicted retained austenite fractions calculated assuming ideal partitioning conditions. In order to calculate these ideal retained austenite fractions, the Constrained Carbon Equilibrium (CCE) was applied [4,5,8]. First, the fractions of untransformed austenite and martensite formed at a given Q_T below M_s were extracted from the dilatometric data as explained in Section 3.1. Assuming that no competing reactions, such as carbide precipitation or austenite decomposition into bainite, are taking place and consequently do not interfere with the partitioning of carbon from the supersaturated martensite to the metastable austenite, the final carbon concentration can then be calculated. The following additional assumptions were made: only carbon can reach a uniform chemical potential, a stationary austenite/martensite interface is assumed and no partitioning kinetics or carbon gradients are incorporated. Based on the final carbon concentrations in the austenite, the new martensite start temperatures M_s were calculated using [28].

As can be seen from Fig. 6a, the optimum quenching temperature is predicted by such a model to be 320 °C, since it leads to a maximum in the austenite volume fraction (17.4%). The austenite fractions after Q & P treatments show significant differences when compared to the calculated values considering ideal partitioning conditions. The measured austenite fractions are found to be less sensitive to the quench temperature and are never larger than the predicted maximum fraction. In Fig. 6a, a maximum of austenite retention at room temperature can be observed for a partitioning time of 120 s when the prior interrupted quench is carried out at 280 °C or 320 °C. However, when quenching at 360 °C, the maximum volume fraction of retained austenite stabilized at room temperature is observed for a partitioning time of 1000 s as can be seen from Fig. 6a.

Regarding the austenite stabilization using austempering, the fraction of retained austenite measured at room temperature increases as the austempering time increases and reaches around 7.2% after 1000 s. As can be observed in Fig. 6b, the maxima of retained austenite at room temperature are reached faster during the quenching and partitioning treatment than during austempering. Indeed, after 120 s of isothermal partitioning or austempering at 400 °C, austenite volume fractions of 11.4% and 5.3% are stabilized, respectively.

3.3. Other transformation products in the microstructures

Although the hypotheses used in the CCE model lead to microstructures consisting only of martensite -fresh and/or tempered- and retained austenite, other transformation products were observed.

Despite the presence of 1.5 wt% of silicon, carbides were detected in martensite laths as can be seen in the SEM and TEM micrographs of Fig. 7. They were identified as ε-carbides by analysis of the corresponding selective area diffraction (SAD) pattern [29]. Such carbon precipitation reduces the carbon available for the partitioning process.

During the partitioning step, expansions were recorded by dilatometry. It was attributed to the formation of bainite [10]. As can be seen in Fig. 8, the dilatations increase when the quenching temperature Q_T increases. As shown by Santofimia et al., the contribution of carbon partitioning to the change in length recorded during partitioning is limited [30]. Assuming that solely bainite transformation accounted for the recorded length changes, it is possible to quantify the fractions of bainite formed during partitioning by using Eq. (2). Furthermore, quenching at a given Q_T below M_s has a strong accelerating effect on the subsequent formation of bainite when compared to the signal

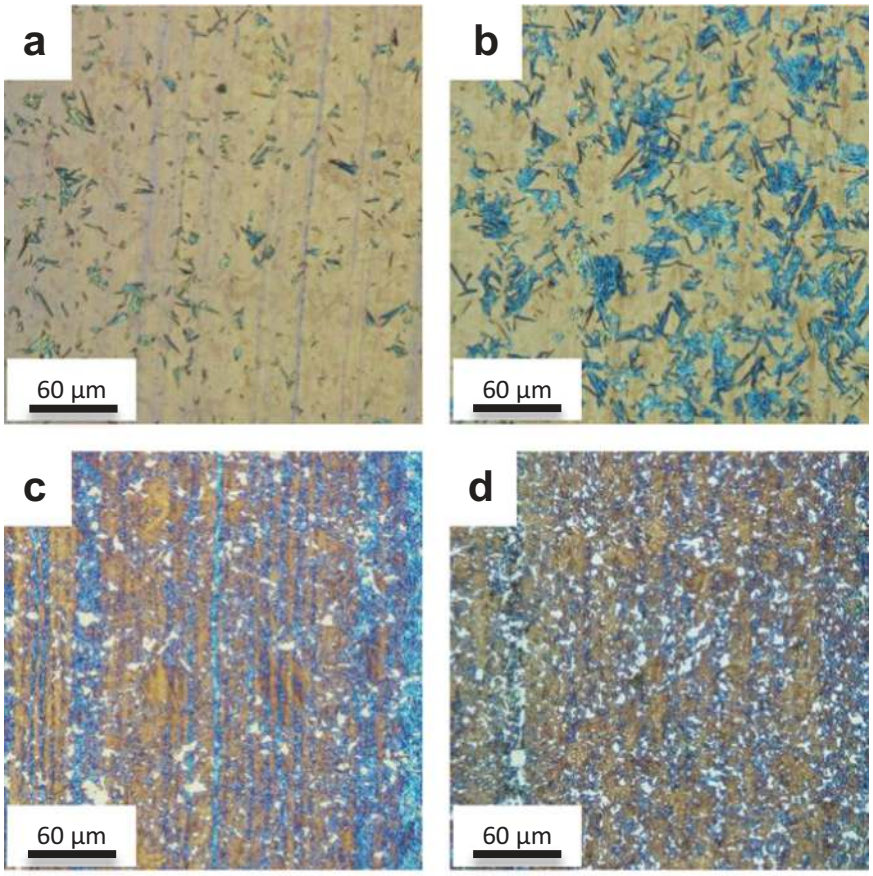

Fig. 3. Optical micrographs using LePera color etching of QAT samples austempered for different times at 400 °C: (a) 30 s, (b) 60 s, (c) 300 s and (d) 1000 s. White areas correspond to retained austenite/fresh martensite islands while blue and light brown areas correspond to bainite.

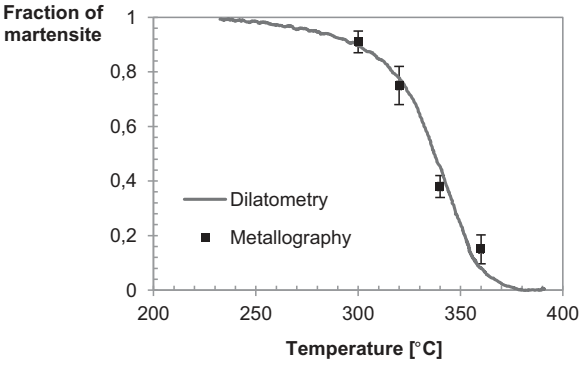

Fig. 4. Martensite volume fractions: 1) estimated using the lever rule on dilatometry curve obtained from continuous cooling – 2) measured using metallography on interrupted quenched specimens.

recorded during austempering. Hence, the volume fractions of bainite formed after 60 s of austempering at 400 °C is 14% while it is 28% for a Q & P sample partitioned at the same temperature after an initial quench at 360 °C.

Depending on the QAT and Q & P parameters, expansions were recorded during the final quench to room temperature and correspond to the formation of fresh untempered martensite from the insufficiently stable austenite. The volume fraction of fresh martensite was quantified using the average grain image quality in EBSD [31]. Indeed, due to its high dislocation content and distorted lattice, fresh martensite is characterized by a poor image quality level in EBSD as observed in Fig. 9. This quantification method is further supported by the comparison of the same area in EBSD and in SEM after conventional Nital etching. The areas exhibiting a low image quality correspond to unetched areas, typical of fresh martensite [26,27]. Furthermore, the obtained volume fractions agree quite well with those that can be calculated from the dilatation recorded during the final quench. Volume fractions of fresh martensite as a function of initial quenching temperature for different isothermal holding times at 400 °C are plotted in Fig. 10. The volume fraction of fresh martensite increases when the quenching temperature Q_T increases and the partitioning time decreases. The largest fractions of fresh martensite are found in the QAT specimens.

The previous detailed characterization methods allowed careful phase quantification in the studied QAT and Q & P microstructures. Fig. 11 summarizes the previous results that were obtained for a fixed holding time of 1000 s at 400 °C by combining the various techniques detailed earlier. As can be observed, when the initial quenching temperature Q_T is decreased from 400 °C to room temperature, the amount of initial martensite in the microstructure increases while the fraction of bainite decreases. Moreover, the formation of fresh martensite during the final cooling to room temperature is hard to avoid when working with high quenching temperatures Q_T and small partitioning times P_t.

3.4. Mechanical properties

In Fig. 12a, the mechanical behavior of a QAT specimen and a Q & P sample are compared. The Q & P sample was initially quenched at 320 °C. Both specimens were isothermally partitioned and austempered at 400 °C for 1000 s. The ultimate tensile strengths of the Q & P and the QAT specimens are found to be similar whereas their yield strengths are significantly different with the yield strength of the Q & P sample being almost 200 MPa higher than the yield strength of the QAT specimen. Consequently, the Q & P sample offers a higher YS/UTS ratio when compared to the QAT specimen. The uniform elongation of the QAT sample is slightly higher than that of the Q & P. Moreover, as can be observed in Fig. 12b, the QAT specimen exhibits a high work-hardening rate at the early plastic deformation stage while the Q & P sample exhibits a clear stage where the n-value increases.

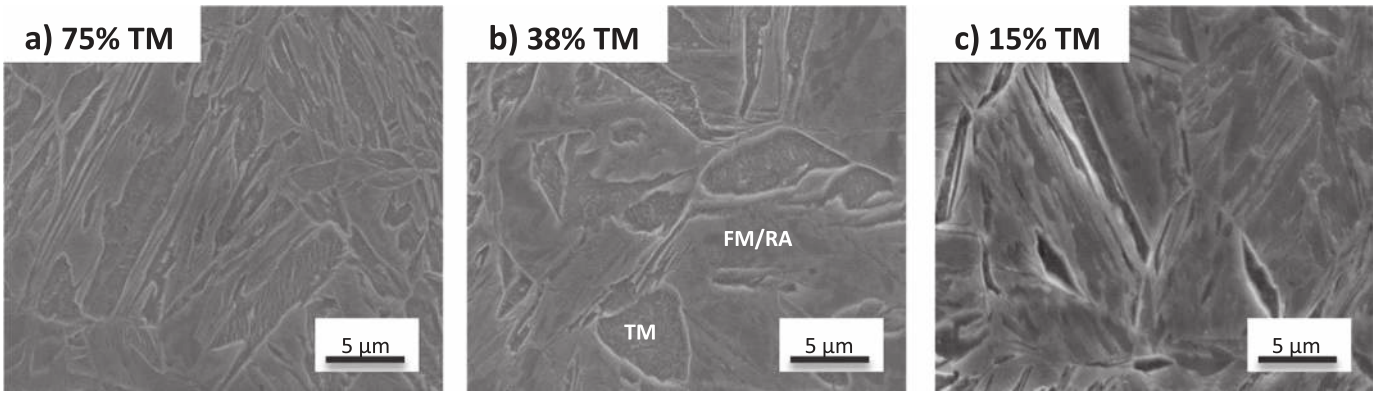

Fig. 5. SEM micrographs of interrupted quenched specimens held at (a) 320 °C, (b) 340 °C, (c) 360 °C for 10 s followed by quenching to room temperature. The etched areas correspond to the auto-tempered martensite (TM) formed at given Q_T while the unetched areas correspond to the untempered fresh martensite/retained austenite (FM/RA) islands formed during the quench to room temperature. Uncertainty of measurements: ± 4%.

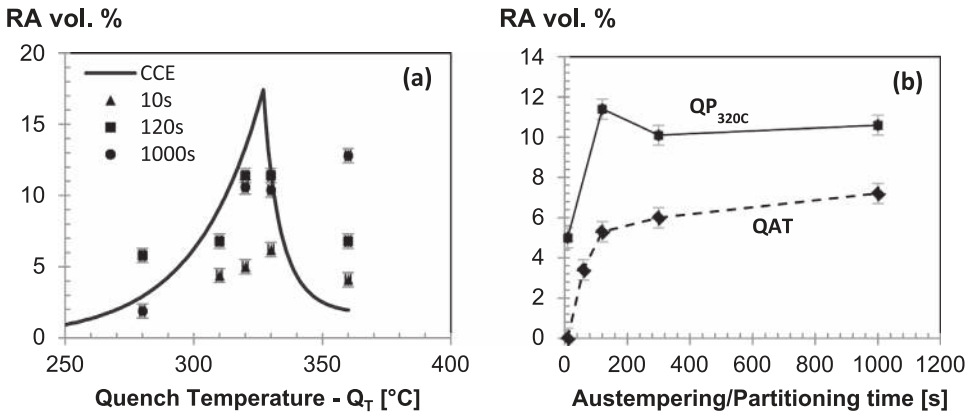

Fig. 6. (a) Retained austenite fractions as a function of quench temperature for Q & P specimens partitioned at 400 °C for different partitioning times (P_t = 10 s, 120 s and 1000 s). The solid curve corresponds to the ideal RA fractions predicted using the constrained carbon equilibrium model. – (b) Retained austenite fractions as a function of isothermal holding time at 400 °C for a Q & P treatment (Q_T = 320 °C) and QAT treatment.

Precise values of the measured mechanical properties and the retained austenite fractions before and after tensile testing can be found in Table 2. So as to offer a complete comparative approach, the mechanical properties of a quenched and tempered (Q & T) specimen are also displayed in this table. The microstructure of such sample consists of almost 100% of tempered martensite. As can be seen, the quenching and tempering treatment results in large strength levels but poor elongation.

The mechanical behavior of various Q & P treated steels obtained with different initial quenching temperatures and various partitioning times are presented in Fig. 13. It can be observed that all stress-strain curves exhibit continuous yielding. Moreover, it can be seen clearly that, for each initial quenching temperature (Q_T = 280 °C, 320 °C and 360 °C), the ultimate tensile strength decreases and the uniform elongation increases with increasing partitioning time. However, the evolution of the 0.2% yield strength with increasing partitioning time

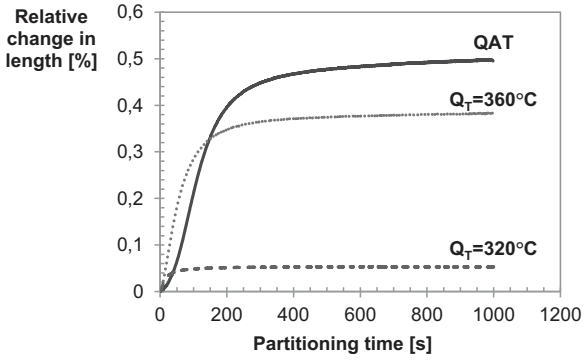

Fig. 8. Changes in length during isothermal holding at 400 °C for QAT specimen and two Q & P samples. The Q & P samples were initially quenched at 320 °C and 360 °C.

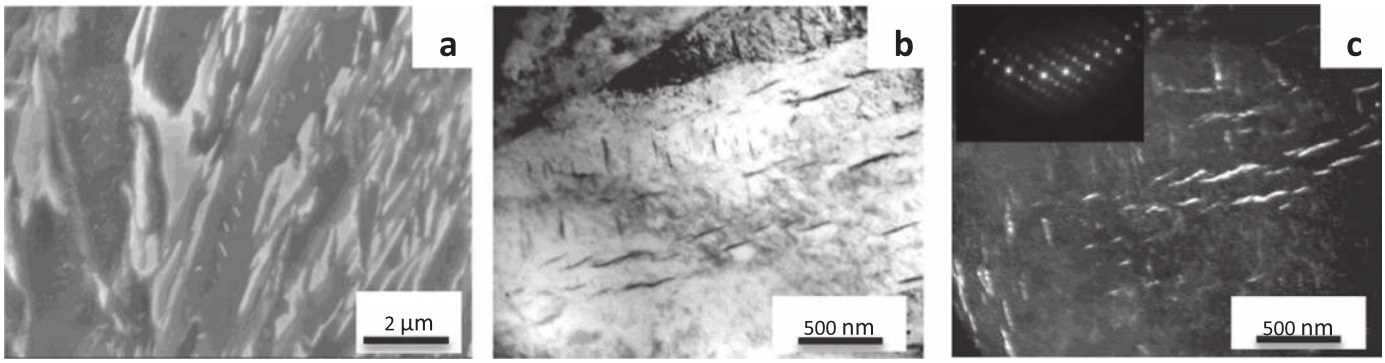

Fig. 7. Carbides in martensite laths: (a) SEM micrograph – (b) TEM bright field image – (c) corresponding TEM dark field image highlighting ε-carbides and corresponding SAD pattern.

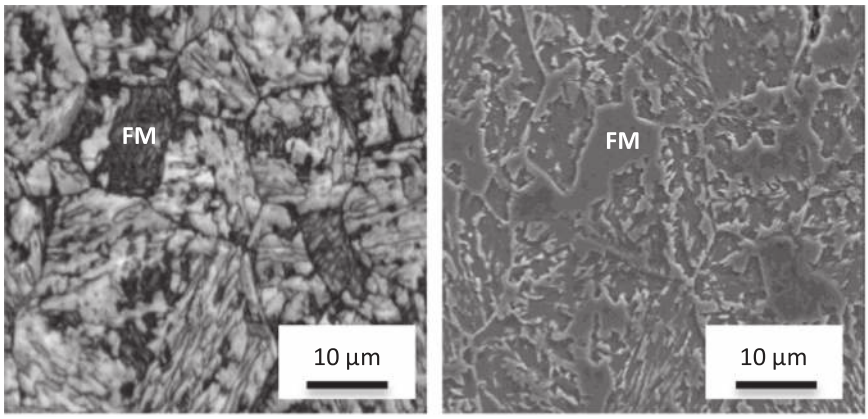

Fig. 9. Observation of fresh martensite in QAT microstructure: (a) EBSD image quality map and (b) SEM micrograph of the same area of the microstructure.

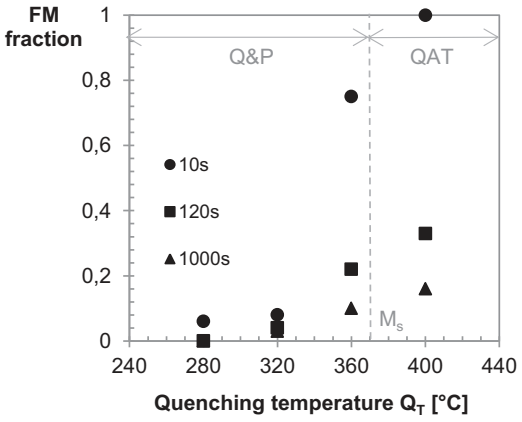

Fig. 10. Volume fractions of fresh martensite in Q & P microstructures treated with different quenching temperatures (280 °C, 320 °C and 360 °C) and various partitioning times (10 s, 120 s and 1000 s) and QAT microstructures obtained with different austempering times (10 s, 120 s and 1000 s). Uncertainty of measurements: ± 0.03.

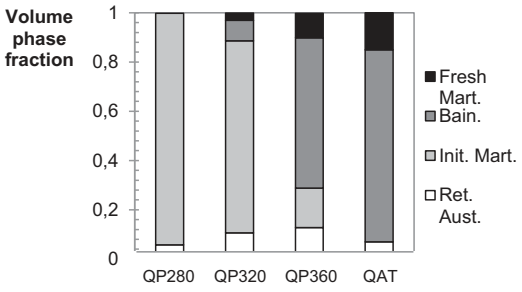

Fig. 11. Volume fractions of retained austenite, initial martensite, bainite and fresh martensite in various Q & P (Q_T = 280 °C, 320 °C, 360 °C) and QAT microstructures held at 400 °C for 1000 s. Uncertainty of measurements: ± 0.04 on initial martensite, ± 0.02 on bainite, ± 0.005 on retained austenite and ± 0.03 on fresh martensite.

depends on the initial quenching temperature. Indeed, when the interrupted quench is carried out at 280 °C or 320 °C, the yield strength slightly increases with partitioning time. On the contrary, when quenching takes place at 360 °C just below M_s, the yield strength clearly decreases with increasing the partitioning time at 400 °C.

Ductility varies with partitioning time as can be observed in Fig. 13b. The uniform elongation is increasing from 6.8% to 9.8% as partitioning time increased from 10 s to 120 s. However, the effect of increasing P_t on ductility is not significant from 120 s to 1000 s. Furthermore, the ultimate tensile strength decreases with partitioning time from 10 s to 120 s, and then stabilizes around 1400 MPa for a fixed quenching temperature of 320 °C.

If we now turn to the evolution of the mechanical properties during austempering (Fig. 14), it is interesting to note that there are clear similarities with the Q & P samples. As observed in Fig. 14, similar observations can be made regarding the influence of austempering time on the mechanical properties of the austempered microstructures: the 0.2% yield strength and the ultimate tensile strength both decrease when increasing the austempering time at 400 °C. The uniform elongation increases with an increasing austempering time.

4. Discussion

4.1. Microstructure development

The final microstructure obtained after the Q & P process is a complex mixture of carbon-depleted martensite, retained austenite, bainite and fresh martensite. The microstructure prior the partitioning step is a controlled mixture of martensite and untransformed austenite formed at a given initial quench temperature Q_T. Therefore, the combination of carbon partitioning, martensite tempering and austenite decomposition into bainite results in complex multiphase microstructures. Metallography solely would not allow clear identification and quantification of Q & P microstructural constituents. The results show that XRD, EBSD and dilatometry techniques need to be combined in order to achieve an in-depth microstructural characterization. This refined

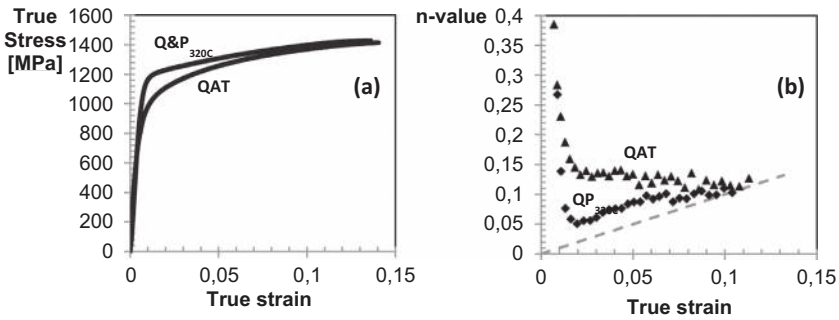

Fig. 12. Comparison of the true stress-true strain curves and strain hardening of the Q & P320C and QAT samples.

Table 2
Mechanical properties (YS = 0.2% yield strength; UTS = ultimate tensile strength; UEl = uniform elongation) and retained austenite fractions (vol%) *before* (RA_{in}) and *after* (RA_{fin}) tensile testing of QAT and Q & P samples. The carbon concentration of the retained austenite is also presented in wt%.

		Time (s)	YS (MPa)	UTS (MPa)	UEl (%)	RA_{in} (%)	C_{conc} (wt%)	RA_{fin} (%)
Tempered martensite (Q & T)		120	1295	1516	2.8	0	–	0
		1000	1290 ± 7	1495 ± 4	3.3 ± 1.1	0	–	0
Q & P	Q_T = 280 °C	10	1010	1463	5.4	0	–	–
		120	1080 ± 8	1390 ± 5	9.8 ± 1.5	5.8	0.98	1.5
		1000	1080 ± 8	1301 ± 4	8.9 ± 1.2	4.0	1.10	–
	Q_T = 320 °C	10	1040 ± 8	1576 ± 6	6.5 ± 1.3	4.7	0.78	1.6
		120	1040 ± 7	1418 ± 5	9.8 ± 1.3	11.5	0.88	2.3
		1000	1070 ± 9	1403 ± 5	10.7 ± 1.2	10.6	0.87	1.5
	Q_T = 360 °C	10	1180 ± 11	1771 ± 7	4.3 ± 1.6	4.1	0.89	
		120	1020 ± 9	1449 ± 5	6.4 ± 1.1	7.0	1.10	2.6
		1000	800 ± 9	1321 ± 4	10.5 ± 1.0	12.8	0.84	1.1
QAT		120	970 ± 9	1510 ± 6	6.8 ± 1.3	5.4	1.05	2.7
		1000	850 ± 8	1379 ± 5	10.9 ± 1.3	7.0	0.82	2.4
		3000	810	1371	11.1	–	–	–

microstructural characterization and quantification allows scrutinizing the relationships between process parameters, microstructures development and resulting mechanical properties. Moreover, direct comparison with the quenching and austempering treatment provides useful additional insights.

As seen in Figs. 2 and 4, the volume fractions of bainite and initial martensite matrices extracted from dilatometry were found to be coherent with the fractions obtained from metallography. It was shown that the volume fractions of the matrices are either time-dependent or temperature-dependent when QAT process or Q & P process is considered, respectively. Indeed, the transformation of 80% of bainite requires austempering during 1000 s at 400 °C while the transformation of the same fraction on initial martensite requires only an interrupted quench at 320 °C.

Furthermore, the stabilization mechanism of metastable retained austenite at room temperature differs between the QAT and the Q & P process. While the carbon enrichment of austenite is achieved through the formation of bainitic ferrite and subsequent C diffusion during austempering, the carbon diffuses directly from the supersaturated martensite into the surrounding austenite during the partitioning step. Unlike austempering, carbon partitioning and microstructure development are decoupled in the Q & P process [7]. Indeed, as can be seen in Fig. 6b, quenching and partitioning results in faster austenite stabilization and, hence, for a given isothermal holding time at 400 °C, lower fresh martensite contents are present in the Q & P microstructure.

In Fig. 6a, the measured retained austenite fractions are compared to the calculated fractions considering ideal partitioning conditions. The CCE model does not consider the kinetics of partitioning or carbon gradients within the austenite and assumes no competing reactions such as carbide precipitation or austenite decomposition into bainite [5,32]. Carbon segregation at dislocations or interfaces and interface migration are not considered in the present work. Competing reactions are taking place during Q & P and explains the lower retained austenite fraction

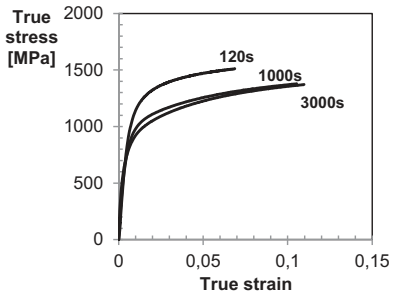

Fig. 14. Effect of austempering time at 400 °C on the tensile properties of austempered samples.

than what was ideally estimated.

Firstly, small fractions of carbides are detected in martensite laths and act as carbon sinks. Even if carbides are detected in the Q & P microstructures, the remaining carbon is sufficiently important to stabilize around 12% of retained austenite. Therefore, the presence of these carbides is not detrimental for Q & P processing as considerable amounts of retained austenite are stabilized.

The formation of bainite during the partitioning step is the second reason of disagreement with the ideal CCE model as it consumes part of untransformed austenite. As highlighted in Fig. 8, the small fractions of bainite formed during the partitioning step are proportional to the quenching temperature, and thus to the amount of untransformed austenite. Moreover, the bainite transformation observed during partitioning is accelerated with the presence of initial martensite. This accelerating effect has been highlighted several times in past literature and is attributed to the additional austenite/martensite interfaces that are acting as nucleation sites [33,34]. When the initial quench is achieved at high Q_T just below M_s, high fractions of unstable austenite are present prior to the partitioning step. In this case, the bainite

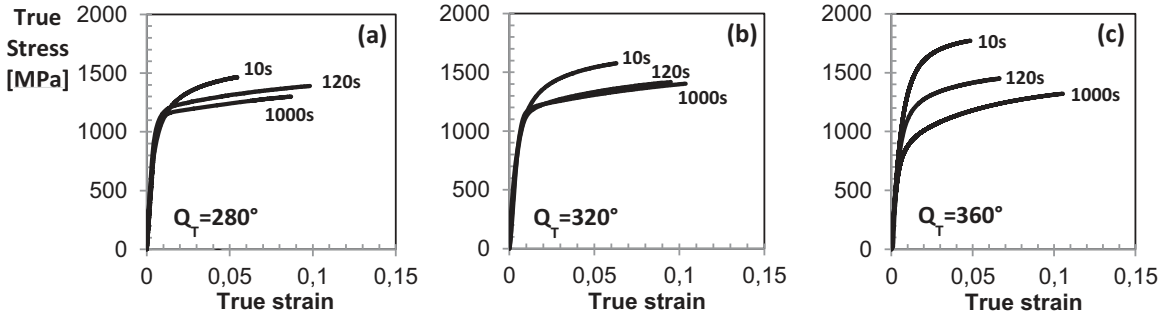

Fig. 13. Effect of partitioning time on the tensile properties of Q & P steels partitioned at 400 °C after quenching at (a) 280 °C, (b) 320 °C and (c) 360 °C. Variations of mechanical properties with partitioning time are more pronounced at higher quenching temperature.

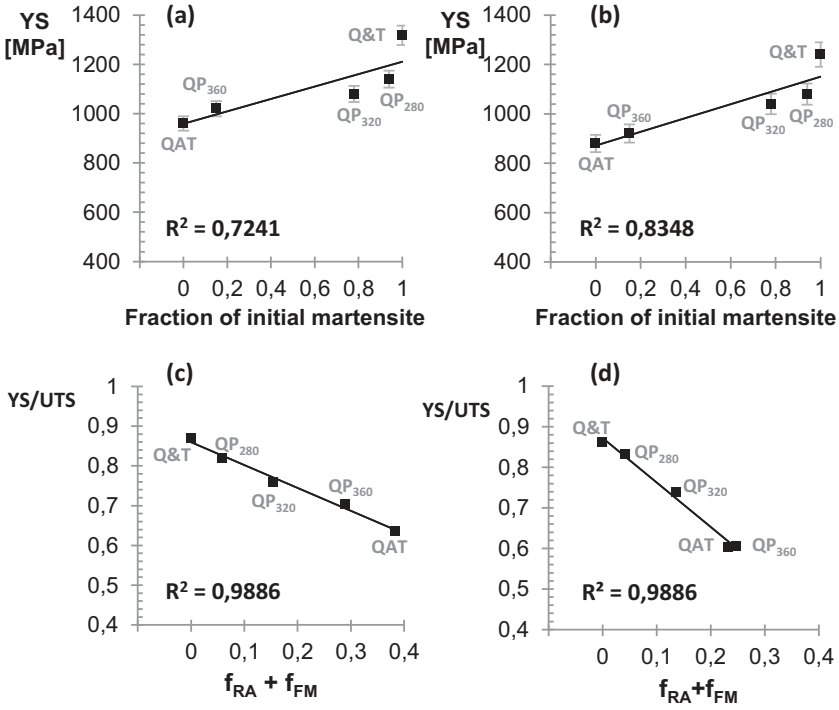

Fig. 15. Impact of Q & P microstructural constituents on the mechanical properties for two different partitioning times: 120 s (Figures (a) and (c)) and 1000 s (Figures (b) and (d)).

formation avoids the formation of significant fractions of untempered fresh martensite during the final quench to room temperature. Indeed, some of the unstable austenite transforms into bainite while, at the same time, carbon-enriching the remaining austenite. Therefore, the partitioning time has to be long enough to avoid formation of fresh martensite during the final quench because the major contribution to the austenite carbon enrichment is provided by the bainitic transformation. As can be seen in Fig. 6a, when quenching takes place at 360 °C, i.e. just below M_s, the maximum of RA volume fraction at room temperature is reached only after 1000 s.

From a general point of view, when the initial quench temperature Q_T is low, such as 280 °C and 320 °C, the principal contribution to carbon enrichment is provided by carbon partitioning from martensite. The maximum RA volume fraction is reached after 120 s of partitioning. On the contrary, when initial quenching is achieved at 360 °C, the austenite decomposition into bainite contributes also to the carbon enrichment of austenite. However, even if bainite is observed in the Q & P microstructures, its fractions is too small to account solely for the measured retained austenite fractions as Clarke and coworkers showed in 2008 [35]. Moreover, as was shown previously, 78% of bainite obtained by austempering for 1000 s stabilizes only 7% of retained austenite. The carbon enrichment of RA is therefore a combination of carbon partitioning and bainitic transformation. The various initial quenching temperatures and partitioning times used in the Q & P process lead to a continuous transition between the quenched and tempered and quenched and austempered microstructures. Indeed, for low Q_T and long P_t, the microstructure mainly consists of tempered martensite. On the other hand, when Q_T is higher, a large fraction of bainite is formed during partitioning like it is the case with direct quenching.

4.2. Mechanical properties

The previous in-depth microstructural characterization and phase quantification allows now scrutinizing the relationships between microstructures development and resulting mechanical properties.

Compared to the QAT specimen, the Q & P samples exhibit a higher 0.2% yield stress. The presence of softer bainitic ferrite compared to the partitioned martensite explains this behavior. As can be seen in Fig. 12a, the ultimate tensile strength and the uniform elongation of the QAT and the Q & P specimens are similar. Regarding the strain-hardening behavior, the QAT specimen exhibits a high work-hardening rate at the early plastic deformation stage. This can be attributed to the hard fresh martensite characterized by its high yield strength. This last still deforms elastically and explains the high initial work-hardening rate. Moreover, the formation of fresh martensite accompanied by a high free dislocation density in the surrounding matrix can also be accounted for the high initial work-hardening rate. The Q & P samples exhibited a clear stage where the n-value increases, owing to a sufficient amount of RA transforming continuously and a carbon-depleted martensite matrix. Indeed, as can be seen in Table 2, the amount of retained austenite considerably decreases during tensile testing of QAT and Q & P specimens. The measured carbon contents of the retained austenite are a clear evidence of the carbon depletion of the martensite matrix.

Even if the evolution of the mechanical behaviors as a function of isothermal holding time at 400 °C is similar in Figs. 13b and 14, the time scale on which these evolutions are occurring is different when comparing Q & P and QAT. Significant decrease in strength and increase in uniform elongation is highlighted from 10 s to 120 s in the Q & P specimen while the same observation can be made from 120 s to 1000 s in the QAT sample. However, when the initial quench in Q & P is achieved at 360 °C, just below M_s, the mechanical characteristics show close similarities with the QAT specimens as only 15% of martensite is formed at this temperature. Major contribution to the microstructural development is provided from the accelerated bainitic transformation as discussed previously.

It has been shown that the yield strength was the most sensitive to the quenching temperature as the latter determines the controlled fractions of initial martensite present in the final Q & P microstructure. Good correlation between the fraction of initial martensite and the yield strength is indeed obtained as can be seen in Figs. 15a and b. Increase in quenching temperature resulted in higher fractions of softer bainite and fresh martensite that both lead to significantly lower yield strength. Indeed, quenching at 360 °C, just below M_s, and partitioning for 120 s led to the formation of 23% of untempered fresh martensite.

Lower ultimate tensile strength with increasing partitioning time was observed because of martensite tempering. The large fractions of fresh martensite at high Q_T and short P_t contributes significantly to the high strengths observed.

The amounts of retained austenite and untempered fresh martensite have a direct impact on the yield ratio YS/UTS. As can be seen in Figs. 15c and d, when the amount of retained austenite and fresh martensite in the microstructure decreases, the yield ratio increases. Low yield ratios are typical for the Q & P steel quenched at 360 °C and the QAT specimen, indicating a free mobility of the dislocations introduced by fresh martensite and transformation of retained austenite into hard martensite during deformation. On the contrary, when the quenching temperature decreases and so the amount of untransformed austenite, the yield ratio approaches the yield ratio of a quenched and tempered steel.

Regarding the uniform elongation levels obtained in the present work, it is difficult to draw clear tendencies with respect to the corresponding microstructures. It is undeniable that the Q & T specimens and Q & P specimens with large fraction of untempered fresh martensite are characterized by poor ductility.

The volume fraction of retained austenite decreases upon straining. However, the exact contribution of the TRIP effect of retained austenite on the uniform elongation still remains unclear [36,37]. Although quenching at 360 °C and subsequent partitioning for 1000 s led to the highest amount of retained austenite, its high content of fresh martensite limits the attained uniform elongation of this specimen [16,17]. In-depth understanding of the interplay between the phases and the uniform elongation still remains a challenge.

Finally, good ductility is achieved by combining a carbon depleted martensite matrix and sufficient amount of retained austenite and by avoiding large fraction of untempered fresh martensite.

5. Conclusions

Q & P was shown to be an effective way for retaining austenite at room temperature. Unlike austempering, the carbon enrichment of the retained austenite and microstructure development are decoupled in the Q & P process. Quenching and partitioning resulted in faster austenite stabilization and, hence, for a given isothermal holding time at 400 °C, lower fresh martensite contents were present in the Q & P microstructure when compared to the QAT microstructure. The resulting Q & P microstructure was a complex mixture of carbon-depleted martensite, retained austenite, bainite and fresh martensite. The fraction of bainite formed during partitioning was shown to be proportional to the amount of untransformed austenite present at the initial quench temperature. At high Q_T, bainite inhibited the formation of large amount of untempered fresh martensite during the final quench to room temperature.

Q & P steels exhibited an interesting balance between strength and ductility. Good correlation between the fraction of initial martensite and the yield strength was obtained. The good ductility was achieved by combining a carbon depleted martensite matrix and sufficient amount of retained austenite and by avoiding large fraction of untempered fresh martensite

Finally, the various initial quenching temperatures and partitioning times used in the Q & P process led to a continuous transition between the quenched and tempered and quenched and austempered microstructures. The achievement of interesting combination of mechanical properties was reached for much shorter processing times compared to QAT steels.

Acknowledgements

The authors acknowledge the CRM and the FNRS for continuous support.

References

[1] M. Ma, H. Yi, Lightweight Car Body and Application of High Strength Steels, in: Y. Weng Y., H. Dong, Y. Gan (Eds.), Advanced Steels, Springer, Berlin, 2011, pp. 187–198.
[2] D.K. Matlock, J.G. Speer, Third generation of AHSS: microstructure design concepts, Microstruct. Texture Steels (2009) 185–205.
[3] E. De Moor, P.J. Gibbs, J.G. Speer, D.K. Matlock, Strategies for third-generation advanced high-strength steel development, AIST Trans. (2010) 133–144.
[4] J.G. Speer, D.K. Matlock, B.C. De Cooman, J.G. Schroth, Carbon partitioning into austenite after martensite transformation, Acta Mater. 51 (2003) 2611–2622.
[5] D.V. Edmonds, K. He, F.C. Rizzo, B.C. De Cooman, D.K. Matlock, J.G. Speer, Quenching and partitioning martensite—A novel steel heat treatment, Mater. Sci. Eng. A 438–440 (2006) 25–34.
[6] J.G. Speer, E. De Moor, A.J. Clarke, Critical Assessment 7: quenching and partitioning, Mat. Sci. Technol. 31 (2015) 3–9.
[7] M.J. Santofimia, L. Zhao, J. Sietsma, Overview of mechanism involved during the quenching and partitioning process in steels, Metall. Mater. Trans. A 42A (2011) 3620–3626.
[8] J.G. Speer, D.V. Edmonds, F.C. Rizzo, D.K. Matlock, Partitioning of carbon from supersaturated plates of ferrite, with application to steel processing and fundamentals of the bainite transformation, Curr. Opin. Solid State Mater. Sci. 8 (2004) 219–237.
[9] M.J. Santofimia, L. Zhao, R. Petrov, J. Sietsma, Characterization of the microstructure obtained by the quenching and partitioning process in a low-carbon steel, Mater. Charact. 59 (2008) 1758–1764.
[10] M.J. Santofimia, T. Nguyen-Minh, L. Zhao, R. Petrov, I. Sabirov, J. Sietsma, New low carbon Q & P steels containing film-like intercritical ferrite, Mater. Sci. Eng. A 527 (2010) 6429–6439.
[11] H.Y. Li, X.W. Lu, X.C. Wu, Y.A. Min, X.J. Jin, Bainitic transformation during the two-step quenching and partitioning process in a medium carbon steel containing silicon, Mater. Sci. Eng. A 527 (23) (2010) 6255–6259.
[12] M.J. Santofimia, L. Zhao, R. Petrov, C. Kwakernaak, W.G. Sloof, J. Sietsma, Microstructural development during the quenching and partitioning process in a newly designed low-carbon steel, Acta Mater. 59 (2011) 6059–6068.
[13] E. De Moor, S. Lacroix, A.J. Clarke, J. Penning, J.G. Speer, Effect of retained austenite stabilized via quench and partitioning on the strain hardening of martensitic steels, Metall. Mater. Trans. A 39 (2008) 2586–2595.
[14] E. De Moor, J.G. Speer, D.K. Matlock, C. Föjer, J. Penning, Effect of Si, Al and Mo alloying on tensile properties obtained by quenching and partitioning, Int. Conf. Mat. Sci. Technol. (MS & T), 2009. p. 1554–1563.
[15] E. De Moor, J.G. Speer, D.K. Matlock, J. Kwak, S. Lee, Effect of carbon and manganese on the quenching and partitioning response of CMnSi steels, ISIJ Int. 51 (2011) 137–144.
[16] E. Paravicini Bagliani, M.J. Santofimia, L. Zhao, J. Sietsma, E. Anelli, Microstructure, tensile and toughness properties after quenching and partitioning treatments of a medium-carbon steel, Mater. Sci. Eng. A 559 (2013) 486–495.
[17] D. De Knijf, R. Petrov, C. Föjer, L.A.I. Kestens, Effect of fresh martensite on the stability of retained austenite in quenching and partitioning steel, Mater. Sci. Eng. A 615 (2014) 107–115.
[18] J. Sun, H. Yu, S. Wang, Y. Fan, Study of microstructural evolution, microstructure-mechanical properties correlation and collaborative deformation-transformation behavior of quenching and partitioning (Q & P) steel, Mater. Sci. Eng. A 596 (2014) 89–97.
[19] Jun Zhang, Hua Ding, R.D.K. Misra, Enhanced strain hardening and microstructural characterization in a low carbon quenching and partitioning steel with partial austenization, Mater. Sci. Eng. A 636 (2015) 53–59.
[20] I. de Diego-Calderón, D. De Knijf, M.A. Monclús, J.M. Molina-Aldareguia, I. Sabirov, C. Föjer, R.H. Petrov, Global and local deformation behavior and mechanical properties of individual phases in a quenched and partitioned steel, Mater. Sci. Eng. A 630 (2015) 27–35.
[21] F.S. LePera, Improved etching technique for the determination of percent martensite in high-strength dual-phase steels, Metallography 12 (1979) 263–268.
[22] J. Durnin, K.A. Ridal, Determination of retained austenite in steel by X-ray diffraction, J. Iron Steel Inst. 206 (1968) 60–67.
[23] B.D. Cullity, Elements of X-Ray Difraction, Addison-Wesley, Reading, MA, 1978, p. 359.
[24] N.H. van Dijk, A.M. Butt, L. Zhao, J. Sietsma, S.E. Offerman, J.P. Wright, S. van der Zwaag, Thermal stability of retained austenite in TRIP steels studied by synchrotron X-ray diffraction during cooling, Acta Mater. 53 (2005) 5439–5447.
[25] S.M.C. van Bohemen, The nonlinear lattice expansion of iron alloys in the range 100–1600K, Scr. Mater. 69 (2013) 315–318.
[26] C.Y. Wang, J. Shi, W.Q. Cao, H. Dong, Characterization of microstructure obtained by quenching and partitioning process in low alloy martensitic steel, Mater. Sci. Eng. A 527 (2010) 3442–3449.
[27] M.J. Santofimia, R.H. Petrov, L. Zhao, J. Sietsma, Microstructural analysis of martensite constituents in quenching and partitioning steels, Mater. Charact. 92 (2014) 91–95.
[28] K.W. Andrews, Empirical formulae for calculation of some transformation temperatures, J. Iron Steel Inst. 203 (1965) 271.
[29] F. HajyAkbary, J. Sietsma, G. Miyamoto, T. Furuhara, M.J. Santofimia, Interaction of carbon partitioning, carbide precipitation and bainite formation during the Q & P process in a low C steel, Acta Mater. 104 (2016) 72–83.
[30] M.J. Santofimia, L. Zhao, J. Sietsma, Volume change associated to carbon partitioning from martensite to austenite, Mater. Sci. Forum 706–709 (2012) 2290–2295.
[31] J. Wu, P.J. Wray, C.I. Garcia, M. Hua, A.J. Deardo, Image quality analysis: a new method of characterizing microstructures, ISIJ Int. 45 (2005) 254–262.
[32] M.J. Santofimia, J.G. Speer, A.J. Clarke, L. Zhao, J. Sietsma, Influence of interface mobility on the evolution of austenite–martensite grain assemblies during

annealing, Acta Mater. 57 (2009) 4548–4557.
[33] A. Navarro-López, J. Sietsma, M.J. Santofimia, Effect of prior athermal martensite on the isothermal transformation kinetics below Ms in a Low-C High-Si Steel, Metall. Mater. Trans. A 47 (2016) 1028–1039.
[34] Y. Toji, H. Matsuda, D. Raabe, Effect of Si on the acceleration of bainite transformation by pre-existing martensite, Acta Mater. 116 (2016) 250–262.
[35] A.J. Clarke, J.G. Speer, M.K. Miller, R.E. Hackenberg, D.V. Edmonds, D.K. Matlock, F.C. Rizzo, K.D. Clarke, E. De Moor, Carbon partitioning to austenite from martensite or bainite during the quench and partition (Q & P) process: a critical assessment, Acta Mater. 56 (2008) 16–22.
[36] P.J. Jacques, J. Ladrière, F. Delannay, On the influence of interactions between phases on the mechanical stability of retained austenite in transformation-induced plasticity multiphase steels, Metall. Mater. Trans. A 32 (2001) 2759–2768.
[37] D. De Knijf, C. Föjer, L.A.I. Kestens, R. Petrov, Factors influencing the austenite stability during tensile testing of Quenching and Partitioning steel determined via in-situ Electron Backscatter Diffraction, Mater. Sci. Eng. A 638 (2015) 219–227.